Transactions of the Materials Research Society of Japan 29[4] 1109-1112 (2004)

Effect of Buffer Layer of Undoped $Bi_4Ti_3O_{12}$ Thin Films Prepared by Metalorganic Chemical Vapor Deposition

Tohru Higuchi, Yuji Hachisu, Makoto Nakamura and Takeyo Tsukamoto
Department of Applied Physics, Tokyo University of Science, 1-3 Kagurazaka, Shinjuku, Tokyo 162-8601, Japan
Fax: 81-3-3260-4772, e-mail: higuchi@rs.kagu.tus.ac.jp

ABSTRACT
The $Bi_4Ti_3O_{12}$ (BIT) thin films with TiO_2 Anataze buffer layer were deposited on the Pt/Ti/SiO_2/Si substrates by metalorganic chemical vapor deposition (MOCVD) method using $Bi(CH_3)_3$ and $Ti(i\text{-}OC_3H_7)_4$ sources. The BIT thin films were crystallized at a low temperature of 500°C. When the total gas flow rate of Ar and O_2 gases was fixed at 180 sccm, the BIT thin films with no-buffer layer and TiO_2 Anataze buffer layer exhibit highly *c*-axis orientation and *a*- and *b*-axes orientations, respectively. The interface between the BIT thin film and the substrate was very smooth. The BIT thin film with TiO_2 Anataze buffer layer consisted of small grain and exhibited a good *P-E* hysteresis loop. Then, the remanent polarization (P_r) was $2P_r$=44.4 μC/cm^2.

Key words: $Bi_4Ti_3O_{12}$ (BIT), metalorganic vapor deposition (MOCVD), buffer layer, TiO_2 Anataze, Bi_2O_3

1. INTRODUCTION

Ferroelectrics $Bi_4Ti_3O_{12}$ (BIT) consists of the layer structure of $(Bi_2O_2)^{2+}$ and has a pseudoperovskite structure along the *c*-axis. The BIT thin films are expected for application to nonvolatile ferroelectric memory (NV-FeRAM) devices with nondestructive readout operation. The BIT has a spontaneous polarization in the *a*-*c* plane at an angle of about 4.5 ° to the *a*-axis, and exhibits two independently reversible components along the *c*- and *a*-axis [1-4]. It shows coercive fields (E_c) of 3.5 kV/cm and 50 kV/cm, remanent polarization (P_r) values of 4.0 μC/cm^2 and 50 μC/cm^2 along the *c*- and *a*-axes, respectively. The large P_r of a-axis takes advantage of reducing the memory cell area of a NV-FeRAM. The formation process at low temperature below 500 °C is desirable for the realization of poly-Si plug stacked capacitor memory cells [5-12]. This is because inter diffusion occurs between the electrode and poly-Si plug during ferroelectric film formation at high temperature. In order to confirm the low temperature deposition of undoped BIT thin films, Kijima and co-workers have proposed two promising buffer layers of BiO_x and Bi_2SiO_5 [5-12] They confirmed that the BiO_x buffer layer effectively lowers the crystallization temperature [5,6]. As a result, the BIT thin films with good crystallinity and ferroelectricity were prepared at 400 °C. Furthermore, they exhibited that the Bi_2SiO_5 buffer layer is also very effective fabricating high quality ferroelectric thin films on Si substrates at low temperature [7-12]. To further investigate the electrical properties and low temperature deposition, it is necessary to perform a more systematic optimizations of the buffer layer.

In the present study, the BIT thin films with TiO_2 Anatase and Bi_2O_3 buffer layers have been prepared on the (111)-oriented Pt/Ti/SiO_2/Si substrate by metalorganic chemical vapor deposition (MOCVD) method. The (111)-oriented Pt layer is most commonly inserted as an electrode between the ferroelectric and insulator layers because of its chemical and thermal stability at high temperature. It has been reported that the TiO_2 Anataze and Bi_2O_3 thin films can prepare at low temperature below 400 °C [13,14]. Therefore, the TiO_2 Anataze and Bi_2O_3 thin films might be promising buffer layer, which can avoid the inter diffusion between BIT thin film and Pt substrate.

2. EXPERIMENTAL

The TiO_2 Anataze buffer layers were prepared on (111) Pt/Ti/SiO_2/Si substrates by MOCVD method. Tetra-isoproxy titanium [$Ti(i\text{-}OCH_3H_7)_4$], which were supplied by TRI chemical Laboratory Inc., used as Ti source of MOCVD. The pressure in the reaction chamber was fixed at approximately 5 Torr. The $Ti(i\text{-}OCH_3H_7)_4$ vaporized in separate stainless-steel bubbler was maintained at 40°C. The substrate temperature (T_s) was approximately 350°C.

BIT thin films were deposited on the TiO_2 Anataze buffer layer prepared on Pt/Ti/SiO_2/Si substrates by MOCVD method using an apparatus having a vertical cold-wall-type reaction chamber [15-18]. Trimethyl bismuth [$Bi(CH_3)_3$] and $Ti(i\text{-}OCH_3H_7)_4$, which were supplied by TRI chemical Laboratory Inc., used as Bi and Ti sources of MOCVD. The $Bi(CH_3)_3$ and $Ti(i\text{-}OCH_3H_7)_4$ vaporized in separate stainless-steel bubblers were maintained at 0°C and 40°C, respectively. The Ar and O_2 gases were used as the carrier gas and the oxidizing gas, respectively. The pressure in the reaction chamber was fixed at approximately 5 Torr. The T_s was fabricated at 500°C in the all BIT thin films. Finally, the top Pt electrodes with a diameter of 0.2 mm were deposited on the film surface through a metal shadow mask by rf-magnetron sputtering in order to measure the electrical properties.

The structural properties of the BIT thin films were characterized by X-ray diffraction (XRD) using CuKα. The surface morphology and cross section was observed by scanning-electron-microscopy (SEM). The electrical properties were measured by using the ferroelectric property measurement system RT-6000HVS manufactured by Radiant Technologies Inc. The polarization-electric field (*P-E*) hysteresis loops were measured using one-shot triangular waveforms with a period of 50 ms.

3. RESULTS AND DISCUSSION

Figure 1 shows the comparison of the composition ratio between as-deposited and post-annealed BIT thin films on $Pt/Ti/SiO_2/Si$ as a function of total gas flow rate. The post-annealed BIT thin films were annealed at 800°C in an O_2 atmosphere for 1 h. Two dashed lines indicate the stoichiometric chemical compositions of Bi and Ti. Open triangle and circle marks are the compositions of Bi and Ti contents in the as-deposited BIT thin films, respectively. Closed triangle and circle marks are the compositions of Bi and Ti contents in the post-annealed BIT thin films, respectively. In as-deposited BIT thin films, the composition ratios indicate Bi-excess and Ti-poor, when the total gas flow rates are 90 and 110 sccm, respectively. In the post-annealed BIT thin films, the composition ratios of Bi and Ti are almost stoichiometric at all total gas flow rates. The apparent difference in composition ratio between the as-deposited and post-annealed BIT thin films is observed at 90sccm. The above results may be the effect of thermal convection at the substrate surface with high substrate temperature.

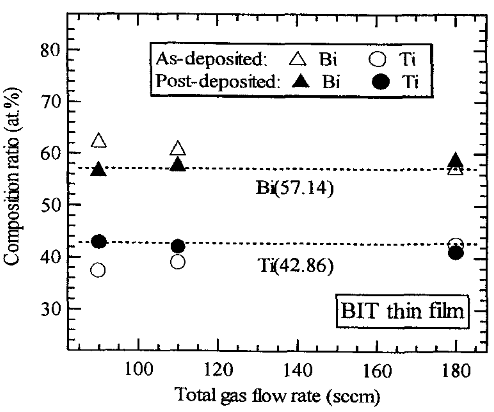

Fig. 1 Comparison ratio of composition ratio between as-deposited and post-annealed BIT thin films deposited at total gas flow rates of 90, 110, and 180 sccm.

Figure 2 shows the comparison of the XRD pattern between the as-deposited and the post-annealed BIT thin films deposited at the total gas flow rates of 90, 110 and 270 sccm. Solid and broken lines denote the pattern of the post-annealed and the as-deposited BIT thin films, respectively. The Pt (111) peak is also observed at 2θ~ 40.0 °. Several closed circles observed in the XRD patterns indicate the existence of the Bi_2O_3 phase. In all as-deposited BIT thin films, the Bi_2O_3 phase is observed at 2θ~27.7 °. The intensity of Bi_2O_3 phase decreases with increasing total gas flow rate. This behavior accords with the result in Fig.1. The existence of the Bi_2O_3 phase is considered to originate from both low-temperature deposition and high deposition rate, though evidence of this has not been clarified in this study. The Bi_2O_3 phase disappears in all post-annealed BIT thin films. The XRD patterns of the post-annealed BIT thin films exhibit BIT single phase, though the existence of the pyrochlore-like phase is observed at 2θ~29.3 ° at a total gas flow rate of 90 sccm. The post-annealed BIT thin films deposited at 90 and 180 sccm exhibit (117)-preferred orientation and *c*-axis proentation, respectively [15,16].

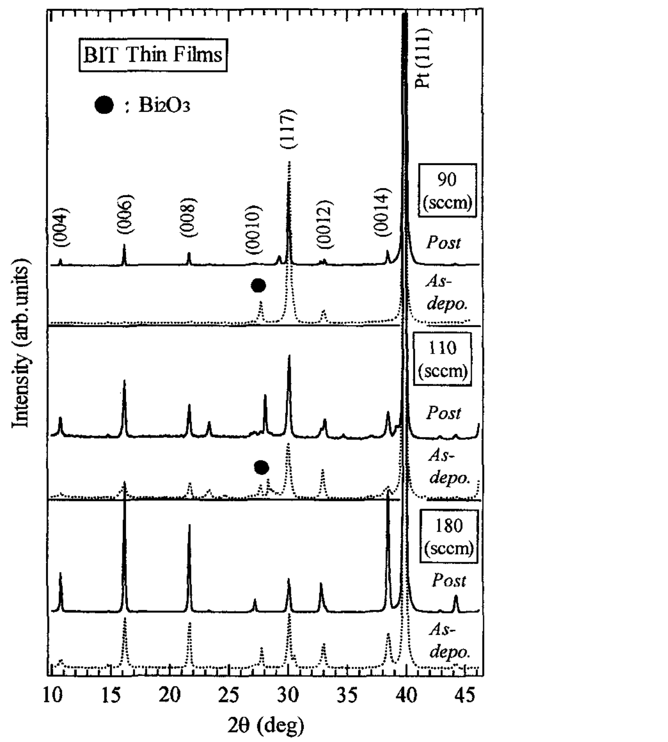

Fig. 2 Comparison ratio of the XRD patterns between as-deposited and post-annealed BIT thin films deposited at total gas flow rates of 90, 110, and 180 sccm.

Figure 3 shows the *P-E* hysteresis loops for the BIT thin film deposited at 90 and 180 sccm. The saturated *P-E* hysteresis loops for the as-deposited BIT thin films were not observed at all total gas flow rates. However, the hysteresis loop of the post-annealed BIT thin film is characterized by a well-saturated *P-E* hysteresis curve. The P_r of post-annealed BIT thin films deposited at 90 and 180sccm were $2P_r$=28.8 μC/cm^2 and 6.42 μC/cm^2, respectively. The coercive fields (E_c) of post-annealed BIT thin films deposited at 90 and 180sccm were $2E_c$=130.7 kV/cm and 118 kV/cm, respectively. The small P_r and E_c of the BIT thin film deposited at 180sccm originate from high *c*-axis orientation, as shown in Fig.2. The dielectric constants (ε_r) of the post-annealed BIT thin films deposited at 90 and 180 sccm were ε_r~330 and 170, respectively.

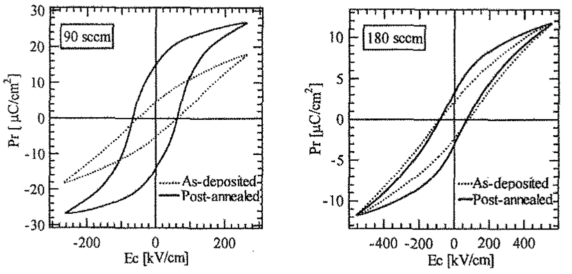

Fig. 3 Comparison of *P-E* hysteresis loops between the as-deposited and post-annealed BIT thin films deposited at 90 and 180 sccm.

Figure 4 shows the XRD patterns of as-deposited BIT thin films with TiO_2 Anataze buffer layer and no buffer layer. As reference, the XRD pattern of as-deposited BIT thin film with Bi_2O_3 buffer layer. The film thicknesses were also approximately 400 nm. The total gas flow rate was fixed at 180 sccm. The composition ratios of Bi and Ti were almost stoichiometry in both films. The existences of Bi_2O_3 and pyrochlore phases are not observed in these XRD patterns. The XRD pattern of BIT thin film with no buffer layer exhibits a highly *c*-axis orientation, though the (117) peaks are observed at $2\theta \sim 30.0$ °. The XRD pattern of as-deposited BIT thin film with Bi_2O_3 buffer layer does not exhibit orientation. In contrast, the XRD pattern of as-deposited BIT thin film with TiO_2 Anataze buffer layer exhibits *a*- and *b*-axes oriented BIT single phase. The mechanism of *a*- and *b*-axes orientation of BIT thin film with TiO_2 Anataze buffer layer can be explained as follows. The lattice parameters of TiO_2 Anataze are a=0.378 nm and c=0.949 nm. The interval of oxygen ions distribution along (101) of TiO_2 Anataze is considered to be relatively close to the *a*- and *b*-axes lattice parameters (0.541nm) more than the *c*-axis parameter (3.283 nm) of BIT. Therefore, the BIT thin film may exhibit the *a*- and *b*-axes orientations on the (101)-oriented TiO_2 Anataze buffer layer.

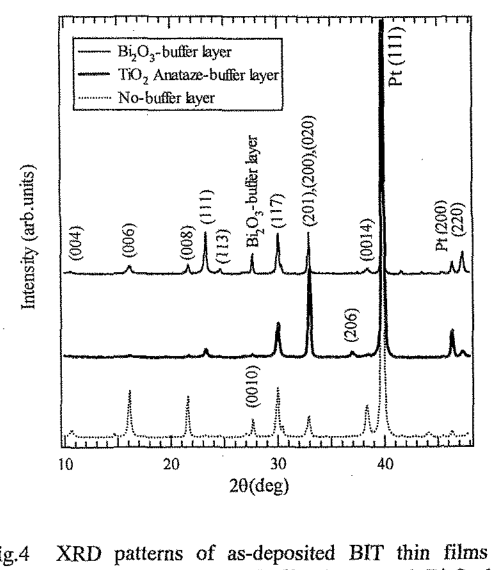

Fig.4 XRD patterns of as-deposited BIT thin films with no-buffer layer, TiO_2 Anatze-buffer layer, and Bi_2O_3 buffer layer.

Figure 5 show the surface morphologies of as-deposited BIT thin films with no buffer layer, Bi_2O_3 buffer layer and TiO_2 Anataze buffer layer. The surface of BIT thin film with no buffer layer and Bi_2O_3 buffer layer exhibit a long or narrow plate-like grain. Furthermore, the existence of pinhole is found. However, the surface of the BIT thin film is improved by using TiO_2 Anataze buffer layer. The grain size of the BIT thin film with TiO_2 Anataze buffer layer is smaller than that of the BIT thin film with no buffer layer. Therefore, one can find that the BIT thin film with TiO_2 Anataze buffer layer is high-density thin film, which consists of small grain.

The cross sectional micrographs of the BIT thin films with no buffer layer, TiO_2 Anataze buffer layer and Bi_2O_3 buffer layer are also shown in Fig. 5. The BIT thin film with no buffer layer and Bi_2O_3 buffer layer consist of well-developed grains with diameters of around 400 nm. The grain shape is isotopic and round. It is also observed from the micrograph that one or two grains are stacked along the out-of-plane direction. On the other hand, the surface and interface of the BIT thin film with TiO_2 Anataze buffer layer are very smooth. These results indicate that the interface structure between BIT thin film and Pt electrode is improved by using TiO_2 Anataze buffer layer.

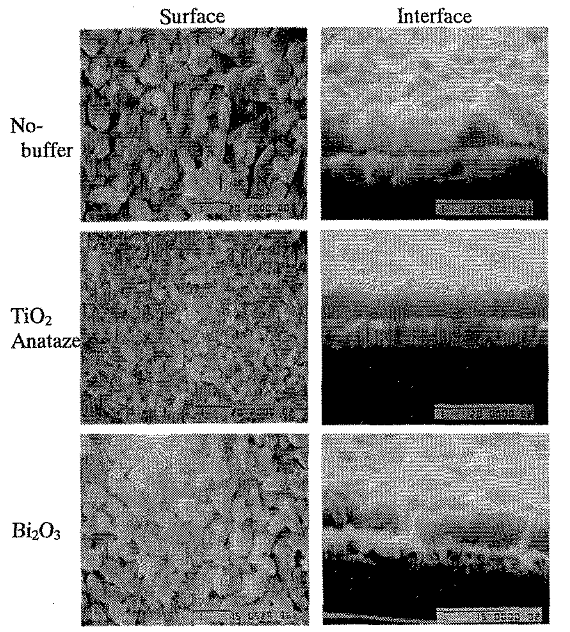

Fig. 5 Surface morphologies and SEM cross-sectional micrographs of as-deposited BIT thin films with no buffer layer, TiO_2 Anataze-buffer layer and Bi_2O_3 buffer layer.

Figure 5 shows the *P-E* hysteresis loop for the BIT thin films with no buffer layer and TiO_2 Anataze buffer layer. These hysteresis loops exhibit good shape. However, the saturated loops were not observed. In particular, the BIT thin films with no-buffer layer and Bi_2O_3 buffer layer contain the effect of leakage current. The P_r and E_c of as-deposited BIT thin film with TiO_2 Anataze buffer layer were 44.4 μC/cm^2 and 276 kV/cm respectively. The large P_r of as-deposited BIT thin film with TiO_2 Anataze buffer layer originates in highly *a*- and *b*-axes orientations. The ε_r of as-deposited BIT thin film with TiO_2 Anataze buffer layer was ~300. The large ε_r of as-deposited BIT thin film with TiO_2 Anataze buffer layer are considered to be due to the oxygen vacancy of TiO_2 Anataze. However, in spite of the low deposition temperature at 500 °C, these thin films have a crystalline structure and ferroelectricity. This fact indicates that the TiO_2 Anataze buffer layer effectively increases the nucleation density and lowers the crystallization temperature of BIT [19].

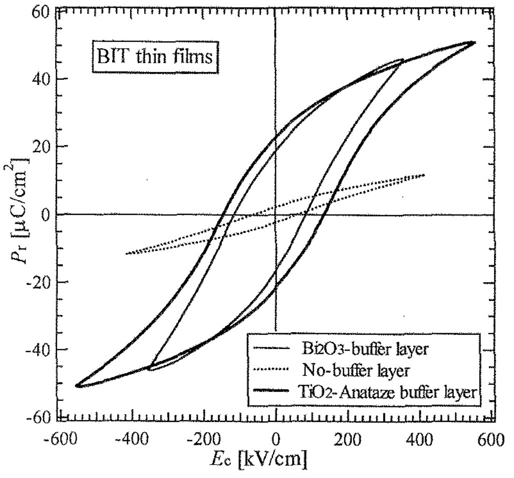

Fig. 5 *P-E* hysteresis loops of as-deposited BIT thin films with no buffer layer, TiO_2 Anataze buffer layer and Bi_2O_3 buffer layer.

4. CONCLUSION

We have studied the effect of buffer layer of BIT thin film on $Pt/Ti/SiO_2/Si$ substrate using MOCVD technique. The BIT thin films were crystallized at low temperature of 500°C. The BIT thin films with TiO_2 Anataze buffer layer exhibit highly *a*- and *b*-axes orientations. Furthermore, the interface structure between BIT thin film and Pt electrode is improved by using TiO_2 Anataze buffer layer. The BIT thin films with TiO_2 Anataze buffer layer exhibit relatively large P_r, which originates highly *a*- and *b*-axes orientations. When the film thickness was fixed at 400 nm, the P_r and E_c of BIT thin film with TiO_2 Anataze buffer layer were $2P_r$ = 44.4 μC/cm^2 and $2E_c$= 276 kV/cm, respectively. Finally, we would like to propose that the TiO_2 Anatase is the promising buffer layer for low temperature MOCVD deposition of BIT thin films.

ACKNOWLEDGEMENTS

This work was partly supported by the Foundation for Promotion of Material Science and Technology of Japan (MST Foundation), Sumitomo Foundation, and a Grant-In-Aid for Science Research from the Ministry of Education, Culture, Sports, Science and Technology of Japan.

REFERENCES

[1] S. E. Cummins and L. E. Cross: J. Appl. Phys. **39** (1968) 2268.
[2] T. Takenaka and K. Sakata: Jpn. J. Appl. Phys. **19** (1980) 31.
[3] R. Ramesh, K. Luther, B. Wilkens, D. L. Hart, E. Wang and J. M. Trascon: Appl. Phys. Lett. **57** (1990) 1505.
[4] H. Esaki: Integrat. Ferroelectr. **14** (1997) 11.
[5] T. Kijima, M. Ushikubo and H. Matsunaga: Jpn. J. Appl. Phys. **38** (1999) 127.
[6] T. Kijima, S. Satoh, H. Matsunaga and M. Koba: Jpn. J. Appl. Phys. **35** (1996) 1246.
[7] T. Kijima and H. Matsunaga: Jpn. J. Appl. Phys. **37** (1998) 5171.
[8] T. Kijima and H. Ishiwara: Jpn. J. Appl. Phys. **41** (2002) L716.
[9] T. Kijima and H. Matsunaga: Jpn. J. Appl. Phys. **38** (1999) 2281.
[10] E. Tokumitsu, T. Isobe, T. Kijima and H. Ishiwara: Jpn. J. Appl. Phys. **40** (2001) 5576.
[11] T. Kijima, Y. Fujisaki and H. Ishiwara: Jpn. J. Appl. Phys. **40** (2001) 2977.
[12] T. Kijima, Y. Kawashima, Y. Idemoto and H. Ishiwara: Jpn. J. Appl. Phys. **41** (2002) L1164.
[13] M. K. Lee, Y. M. Hung and J. J. Huang: Jpn. J. Appl. Phys. **40** (2001) 6543.
[14] E. K. Kim, M. H. Son, S. K. Min, Y. K. Han, C. H. Wang and S. S. Yom: J. Appl. Phys. **79** (1996) 4459.
[15] M. Nakamura, T. Higuchi and T. Tsukamoto: Jpn. J. Appl. Phys. **42** (2003) 5687.
[16] M. Nakamura, T. Higuchi and T. Tsukamoto: Jpn. J. Appl. Phys. **42** (2003) 5969.
[17] T. Watanabe, H. Funakubo, K. Saito, T. Suzuki, M. Fujimoto, M. Osada, Y. Noguchi and M. Miyayama: Appl. Phys. Lett. **81** (2002) 1660.
[18] T. Watanabe, H. Funakubo, M. Osada, Y. Noguchi and M. Miyayama: Appl. Phys. Lett. **80** (2002) 100.
[19] M. Nakamura, T. Higuchi, Y. Hachisu and T. Tsukamoto: Submitted to Jpn. J. Appl. Phys.

(Received October 11, 2003; Accepted March 10, 2004)